



Research paper

The oral cavity as a biological barrier system: Design of an advanced buccal in vitro permeability model

Birgit J. Teubl^a, Markus Absenger^b, Eleonore Fröhlich^b, Gerd Leitinger^{b,c}, Andreas Zimmer^a, Eva Roblegg^{a,d,*}

^a Institute of Pharmaceutical Sciences, Department of Pharmaceutical Technology, Karl-Franzens University, Graz, Austria

^b Center for Medical Research, Medical University of Graz, Austria

^c Institute of Cell Biology, Histology and Embryology, Medical University of Graz, Austria

^d Research Center Pharmaceutical Engineering, Graz, Austria

ARTICLE INFO

Article history:

Available online 3 January 2013

Keywords:

Buccal mucosa
In vitro model
Animal mucin
TR 146 cells
Nanoparticles

ABSTRACT

An important area for future research lies in finding a drug delivery system across or into the oral mucosa. However, to design such systems, simplified biological models are necessary so that the mechanisms and/or interactions of interest can readily be studied. The oral epithelium is covered by a complex mucus layer, which enables exchange of nutrients and provides lubrication. However, it has been demonstrated that mucus has an impact on the mobility of nanoparticles and drug molecules. Thus, we aimed to develop an advanced buccal in vitro model for studying transport of nanoparticles, taking the mucus layer into account. First, animal mucins (porcine gastric, bovine submaxillary) were compared with natural human mucin regarding chemical and morphological structure. Second, an “external” mucus layer was prepared by a film method and deposited onto an oral cell line (TR 146), cultured on transwells[®]. Adherence of the mucin fibers was evaluated and the viability of the model was assessed. Nanoparticle transport studies were performed with this advanced in vitro model and an ex vivo diffusion system. The results revealed that porcine mucin is most similar to human natural mucin in chemical structure and morphology. Both the bovine and porcine mucin fibers adhered onto the oral cells: Due to the different morphology of bovine mucin, the viability of the oral cells decreased, whereas porcine mucin maintained the viability of the model for more than 48 h. Comparison of in vitro data with ex vivo data suggested reliability of the advanced buccal in vitro model. Additionally, it was demonstrated that the mucus layer in the oral cavity also acts as a strong barrier for the mobility of nanoparticles.

© 2012 Elsevier B.V. All rights reserved.

1. Introduction

The most commonly used route in drug delivery is oral administration with intestinal absorption. The majority of solid dosage forms is placed in the mouth and is expected to be swallowed. However, this has several significant disadvantages, including enzymatic degradation of the drug in the stomach and the intestine, as well as hepatic first pass metabolism. As such, other drug delivery sites are considered as an alternative route for the delivery of therapeutic agents [1]. Together with the nasal passage, pharynx, and urogenital region, the oral cavity is part of the oral mucosa and provides an interesting target site for local and systemic drug delivery [2]. Several intraoral dosage forms have been developed,

including sublingual and rapid-melt tablets, (mucoadhesive) films, (lyophilized) wafers, patches, bioerodible disks, and microparticles (see e.g., [3–5]). Generally, these dosage forms can be classified according to their dissolution and/or disintegration kinetics as quick-dissolving (QD), slow-dissolving (SD), or non-dissolving (ND) systems [6]. QD systems disintegrate within a few seconds to a minute upon contact with saliva without the need of water or chewing. They provide several benefits, including enhanced efficacy and convenient administration (especially for patients suffering from dysphagia) resulting in an improved patient compliance. SD systems also dissolve in the oral cavity within 1–10 min, whereas ND systems do not dissolve entirely and are therefore appropriate systems for controlled drug delivery. However, the extent of buccal drug absorption, including penetration/permeation, is determined by the physicochemical properties of a drug and is important for pharmacokinetics and hence the pharmacological action of the drug. New pharmaceutical formulations that apply nanoparticles (NPs) can improve drug delivery in the oral cavity. Yet their design is often impeded by a lack of understanding of

* Corresponding author. Institute of Pharmaceutical Sciences, Department of Pharmaceutical Technology, Karl-Franzens University, Humboldtstrasse 46, A-8010 Graz, Austria. Tel.: +43 316 380 8888; fax: +43 316 380 9100.

E-mail address: eva.roblegg@uni-graz.at (E. Roblegg).

how they interact with biological tissues; thus, buccal *in vitro* permeability models are necessary.

The oral cavity is covered by a stratified squamous epithelium, which can be divided into two types [7]: keratinized and non-keratinized epithelium. Keratinized epithelium covers areas of masticatory mucosa, such as the hard palate and gingiva. The surface is inflexible, tough, and resistant to abrasion. The non-keratinized epithelium covers areas of the lining mucosa, which is present on the lips, the buccal mucosa, alveolar mucosa, soft palate, the floor of the mouth, and underside of the tongue. Compared with the keratinized epithelium, it is thicker and shows tolerance to compression and distention due to accommodate chewing, swallowing, and speech. Delivery of drug molecules into or across the buccal mucosa requires penetration into the superficial layers before a local or systemic effect can be obtained. The degree of permeability is least in the gingival mucosa, followed by the buccal mucosa. The most easily permeated area is the sublingual mucosa (i.e., floor of the mouth). Nevertheless, this region is permanently washed by saliva making drug delivery difficult [8]. The buccal mucosa, in contrast, represents a large surface area (23% of the total surface of the oral mucosa including the tongue) and is more fitted for systemic drug delivery [7,9,10]. Consequently, this study focuses on the buccal region of the oral cavity.

To study buccal mucosal permeability of drug loaded nano-carrier systems so far, three approaches have been used: (i) *in vivo* studies, (ii) *ex vivo* experiments, and (iii) *in vitro* systems. One of the simplest methodologies to study penetration/permeation in living human organisms is the buccal absorption test, also known as swirl and spit test [11]. However, there are some drawbacks. On the one hand, the accuracy of the experiments is limited by the sensitivity of the equipment to evaluate drug concentration, and on the other hand, information about the permeability/penetration into/through different areas of the oral cavity is not provided. Another method is the so-called “*in vivo* perfusion,” which is commonly used in pharmacokinetics [12]. Perfusion experiments are carried out with perfusion chambers attached onto various sites of the oral cavity. Drug solutions are circulated in the device and collected at different time points. One disadvantage here is that local drug metabolism can only be considered when intravenous infusion experiments are performed too. Frequently, animal models are preferred systems, although they often show different results when applied to humans [13].

The most commonly used *ex vivo* methods are carried out with static and dynamic permeability chambers. A variety of tissues from sacrificed animals can be used for oral mucosal permeability studies. Due to morphological similarities, buccal mucosa of the pig has been considered as an appropriate model of human buccal mucosa for drug permeability studies [14,15]. However, one important aspect of these systems is to maintain the activity of the protective barriers that prevent the movement of xenobiotics in the buccal mucosa. These barrier systems depend on the tissue homeostasis (and in series on the ATP content), the tissue integrity, the cell morphology, aging processes, and/or diseases as well as on the viability [2]. Studies by Wertz and Squier [16] revealed that the membrane coating granules (MCGs), which display the principle penetration barrier to the movement of particles, spread their lipid content into the intercellular space. This process only occurred in viable cells with biochemical active organelles. The viability of the buccal mucosa of the pig, for example, can only be maintained for 6–8 h [17], and thereafter, it decreases significantly.

In vitro studies addressing permeation usually use transwells® systems, where cells are (co-) cultured on filters [18–20]. The TR146 cell line has been proposed as a model of human buccal epithelium [21]. These cells originate from a neck node metastasis of a human buccal carcinoma [22]. Jacobson et al. and Nielsen and Rassing [21,23] demonstrated in their studies that this cell line is

appropriate to study the permeability behavior of selected markers and/or active pharmaceutical ingredients (APIs). However, Nielsen and Rassing [24] also showed that mannitol and testosterone permeated the TR146 cell culture model ten times faster than human buccal mucosa. These data reveal that one cell line cannot replicate the anatomical and physiological complexity of the tissue. Additionally, it is known that mucus can also pose a potential barrier to drug/nanoparticle absorption [25].

The buccal mucosa has a thickness of approximately 500–800 μm [16]. It consists of a mucus layer, the stratum-superficiale, the stratum-spinosum and the stratum-basale (i.e., 40–50 cell layers). Underneath the epithelium, the lamina propria can be found, consisting of connective tissue with a network of blood vessels, many capillaries, and smooth muscles [9]. The buccal mucosa shows a variety of functions of which the protection of the underlying tissue, and thus, avoidance of the penetration/permeation of xenobiotics is the most important one. Hence, a variety of barrier mechanisms are integrated in this part. The first decisive player in the oral cavity is the saliva, produced by sublingual and by salivary glands. The pH of the saliva is slightly acidic (5.8) in rest and goes up to 7.6 when stimulated [26]. It mainly consists of water (95–99% per weight), enzymes, inorganic salts, lipids, and glycoproteins, so-called mucins. MG1, a high molecular weight mucin composed of disulfide-linked subunits, is able to adhere to the surface of the oral epithelium and constitutes the second penetration barrier, the mucus layer [27–30]. This “external” layer is a three-dimensional network with high water holding capacity. The average thickness, calculated from the residual volume of saliva after swallowing (0.77 ml), the volume before swallowing (1.07 ml) as well as the total surface area of the adult human mouth ($214.7 \pm 12.7 \text{ cm}^2$), varies between 70 and 100 μm [10,31]. It is known that the main penetration barrier for drug molecules lies in the top third region of the epithelium [32]. This is due to the fact that the cells increase in size and become flatter as they get from the basal layers to the superficial layers. The time to replace the cells in the buccal epithelium, that is, the turnover time, is derived from knowledge of the time it takes for the cell to divide and pass through the epithelium. Data from the median turnover time in the buccal mucosa range from 6 to 14 days [9,33]. Another permeability barrier is the intracellular material, derived from the MCG in the 200 μm outermost part of the superficial layer [34,35]. These granules are small structures containing glycolipids. MCGs produce “lipid contents” during differentiation and discharge them into intercellular spaces. Thereby, they constitute a permeability barrier and thus limit the penetration of non-polar groups.

To achieve a basic understanding of cellular and sub-cellular functions, an *in vitro* culture model including a mucus layer was developed. The advanced buccal *in vitro* monolayer model composed of oral epithelial cells (TR 146), cultured on transwells®, and of an “external” mucus layer, which was prepared by a film method. The layer was deposited onto the cells, and adherence of the mucin fibers onto the cells was evaluated. Furthermore, the viability of the model was investigated and the transport of polystyrene nanoparticles was studied and compared with *ex vivo* experiments to ensure reliability of the *in vitro* model.

2. Materials and methods

2.1. Human versus animal mucins

Lyophilized mucin from porcine stomach and mucin from bovine submaxillary glands were obtained from Sigma-Aldrich (Munich, Germany). Human saliva was collected from 10 male and female healthy donors (Austrians, aged between 25 and 45 years, non-smoker) as previously described by Park et al. [36] and centri-

fused for 1 h at 425g (Eppendorf Centrifuge 5415 R). The supernatant fluid was immersed into liquid nitrogen (-196°C) for 15 min and transferred into a freeze drier (LYOVAC GT 2). After vacuum was applied, the mucin was dried for 48 h at ambient temperature. To evaluate if animal mucins show chemical and morphological similarities to human mucin, scanning electron microscopy (Zeiss DSM 950) and Fourier transform infrared spectroscopy (FTIR) were performed. FTIR was conducted using a Bruker VERTEX 70 instrument, equipped with a DLATGS-detector, in the 2000–600 cm^{-1} region. Thereby, a close contact of the samples with the diamond ATR crystal was ensured. The spectroscopy measurements were an average of 16 scans, where the baseline was corrected. Viscosity measurements were conducted with a Physica MCR 301 rotational rheometer (Anton Paar) using cone-plate geometry (CP 50-1). The shear rates ranged between 100 s^{-1} and 300 s^{-1} . All tests were performed with 570 μl sample volume of mucin dispersion (100 mg/ml) at room temperature threefold.

2.2. Preparation of the external mucus layer

Mucin was dispersed in distilled water (100 mg/ml) and sonicated for 10 min at room temperature. To increase the flexibility and avoid brittleness of the layer, glycerol (1–10%) was added as plasticizer in different concentrations. Prior to use, the mucin dispersion was sterilized by autoclaving (Astell Scientific). To prevent bacterial contamination, all preparation steps were carried out under aseptic conditions. A 800 μl sample volume of the mixture was filled into a plastic ring (a bottomless transwell[®]), which was fixed on a foil (area 1.131 cm^2), and dried for 10 days at 4 $^{\circ}\text{C}$, 37 $^{\circ}\text{C}$, room temperature, and laminar flow air, respectively. The dried mucus layers were then gently removed from the ring and the foil with a microtome blade. The layers were stored under aseptic conditions.

2.3. Scanning electron microscopy (SEM)

To evaluate the network structure and the mesh size of the mucin layers and the human mucin, the samples were re-suspended in 500 μl Milli-Q water onto poly-L-lysine coated cover glasses. Fixation was carried out in Schaffers fixative (37% formol/100% ethanol) for 2 h to maintain the native mucin structure [37]. Subsequently, dehydration was carried out through a graded series of ethanol (80–100%). This was followed by critical point drying (Bal-Tec CPD O30) and gold palladium sputtering (Bal-Tec SCD 500). The samples were coated at 25 mA for 60 s under argon atmosphere and examined in a scanning electron microscope (Zeiss DSM 950).

2.4. Cell culture

The TR146 cells, which were obtained from Imperial Cancer Research Technology (London, UK), were grown in DMEM with supplements of 10% FBS, 200 μM L-Glutamine, 100 IU/ml penicillin, and 100 $\mu\text{g}/\text{ml}$ streptomycin. The H376 cell line from Sigma-Aldrich (Vienna, Austria) was grown in DMEM/HAMS F12 (Nutrient mixture F 12) (1:1), supplemented with 10% FBS, 200 μM L-Glutamine, and 0.5 $\mu\text{g}/\text{ml}$ sodium hydrocortisone succinate. Briefly, culture conditions were maintained at 37 $^{\circ}\text{C}$ in 98% humidity of 5% CO_2 /95% air. Sub-cultivation was performed at approximately 70% confluence with 0.25% trypsin–EDTA. Prior to use, cells were cultured on 1.131 cm^2 permeable Corning Costar[®] 12 well inserts (polycarbonate filters; Szabo Scandic, Vienna, Austria) with a pore size of 3.0 μm . The seeding density was 2.4×10^4 cells/ cm^2 , and the incubation time was 30 days. The transepithelial electrical resistance (TEER) was measured with an Endohm culture cup

connected to an EVOM voltohmmeter (World Precision Instruments). Cell morphology was investigated via SEM.

2.5. Mucus adherent effects

The external mucus layer was deposited onto the confluent TR 146 cell layer (28 days in culture) and incubated for 24 h at 37 $^{\circ}\text{C}$. The visualization of the mucus adherent effects onto the cell surface was conducted by using SEM and laser scanning microscopy (LSM). The samples were washed twice with 500 μl Hank's Buffered Salt Solution (HBSS), fixed with Schaffers fixative, and dehydrated in an ethanol series (80–100%). After critical point drying and gold palladium sputtering, the samples were analyzed in a scanning electron microscope. Acridine Orange (Sigma–Aldrich) was used for fluorescent labeling of the cells and the mucoglycoproteins. The cell medium was replaced with HBSS/Acridine Orange (2 mg/ml) and incubated for 10 min at 37 $^{\circ}\text{C}$. Subsequently, the cells were washed twice with 0.5 ml HBSS. The membrane was removed with a scalpel blade from the transwell[®] insert and mounted on a slide. Images were monitored with a fluorescence microscope (Axio Observer, Zeiss; camera: Axio Cam) at 546/12 nm excitation wave length using a BP 575–640 nm band pass detection for the red channel and 470/40 nm excitation wave length in conjunction with BP 525/50 for the green channel.

2.6. Formazan bio-reduction

In order to examine the viability of the advanced model, a CellTiter 96[®] Aqueous Non-Radioactive Cell Proliferation Assay (Promega) was used according to the manufacturer's instructions. 2×10^4 cells/200 μl medium were seeded in a 96 well plate and cultured for 24 h. Subsequently, the medium was replaced with aliquot parts of the mucus layer/serum-free medium ($n = 6$) and incubated for 4, 24, and 48 h. 20 μl of a MTS/PMS solution per well was added and re-suspended. After an incubation time of 4 h, the absorbance was measured at 490 nm with a VIS-plate reader (FLUO-Star Optima, BMG, Labor-technik).

2.7. In vitro nanoparticle transport studies

Red (580/605) fluorescence-labeled carboxyl polystyrene (CP) particles of 200 nm and red (580/605) fluorescence-labeled amine modified polystyrene (AP) particles (FluoSpheres[®]) were purchased from Invitrogen (Darmstadt, Germany). Red fluorescence-labeled (542/612) plain polystyrene (PP) particles of 200 nm were purchased from Fisher Scientific (Vienna, Austria). The transport studies were performed with the advanced in vitro model at 37 $^{\circ}\text{C}$. 0.5 ml of a polystyrene particle/phosphate buffered saline (PBS) dispersion was applied to the apical side in a concentration of 100 $\mu\text{g}/\text{ml}$. The cell nuclei were stained with 1 $\mu\text{g}/\text{ml}$ Hoechst 33342 (Invitrogen). To determine the particle transport after 4 h, the filters were washed twice with 0.5 ml PBS and the removed membrane was mounted on a slide. Images were acquired with a LSM510 Meta confocal laser scanning microscope (Zeiss) with 405 nm/BP 420–480 nm for the blue channel and 543 nm/LP 560 nm for the red channel. Afterward, z-stacks were acquired and virtual radial sections were documented.

2.8. Ex vivo nanoparticle transport studies

The transport of the nanoparticles through porcine buccal mucosa was investigated using static Franz diffusion cells (PermeGear, Hellertown, USA). The receiver compartment was filled with 7.8 ml PBS buffer at 37 $^{\circ}\text{C}$. The excised buccal mucosa (Karnerta Slaughter House, Graz, Austria) was mounted between the donor and receptor compartments and pre-equilibrated with 1 ml PBS buffer.

Subsequently, the buffer was replaced with 200 mM CP, AP, and PP particles dispersed in PBS in a concentration of 100 $\mu\text{g}/\text{ml}$. After 4-h incubation time, the mucosa was washed three times with PBS and fixed in 4% formalin. The samples were shock-frozen in Neg-50 Kryo-Media and cut into 10 μm slices with a cryo-microtome (Microm HM560). The samples were investigated using fluorescence microscopy (Olympus BX-51, camera: DP-71). Images were acquired with excitation BP 520–550 nm and emission LP 580 nm for red fluorescence.

3. Results and discussion

3.1. Characterization of animal and human mucins

The mucin family comprises 20 members, which are divided into two groups: the secreted soluble mucins (SSMs) and the membrane-associated mucins (MAMs) [38,39]. The expression as well as the functions of MAM in the oral cavity is less well understood. They include MUC1, MUC4, and MUC16, which are produced in the parotid and the submandibular and also in the minor salivary glands. The secreted mucin MUC5B is produced by all salivary glands except the parotid [40,41], and the soluble MUC7 is produced by the submandibular, the sublingual, and the parotid glands [42]. Their roles on the mucus network formation are not well known. However, the development of a physiological buccal permeability *in vitro* model requires an understanding of the structure of this protective mucus gel, which covers the epithelial cells. To evaluate which materials mimic the structural and morphological properties of natural human mucin, various saliva substitutes administered to xerostomic patients (saliva production is diminished) were investigated [43,44]. Previous studies have reported that (animal) mucin based substitutes are more effective than carboxymethyl-cellulose based saliva substitutes [45]. In this study, animal mucins, including porcine gastric and bovine submaxillary, were evaluated regarding their chemical and morphological similarities to natural human mucin. The chemical properties were measured with FTIR, which provides information about the secondary structure contents of proteins (mucins). A high similarity between the absorption spectra of bovine submaxillary, porcine gastric, and human salivary mucin was seen (Fig. 1). The appearance of the Amide I and Amide II bands, which are the characteristic sets of absorption bands (i.e., 1647 cm^{-1} and 1541 cm^{-1}) for proteins [46], was essentially identical in all tested mucins. Since the Amide I frequency is associated with the protein structure, our data led to the assumption that the mucins exhibited an unordered secondary structure (frequency range between 1640 and

1648 cm^{-1}), which could include turns, random coils, and extended secondary structure elements [47].

Apart from the chemical structure, the morphological structure of the mucin fibers was studied by SEM (Fig. 2). Pig gastric mucin (Fig. 2a) showed a high similarity to human mucin (Fig. 2c). However, bovine submaxillary mucin (Fig. 2b) formed thicker fibers that agglomerated. These data are supported by findings of Bettelheim and Dey [48]. They observed that at low ionic strength, bovine submaxillary mucin is a rigid rod. With increasing ionic strength, the molecule becomes a stiff and compact coil. Moreover, porcine gastric mucin comprises MUC5AC and MUC6, two gel forming mucins [49], and MUC1 and MUC16, two cell surface mucins. Compared with the oral cavity, MUC5AC shows high similarities to the salivary mucin MUC5B [50], and MUC1 and MUC16 are also available in the oral cavity [51]. These findings suggest that human mucin can be modeled by porcine gastric mucin.

3.2. Preparation and characterization of the external mucus layer

In the oral cavity, the mucus layer is formed by mucins of the saliva instead of mucus-secreting cells. To simulate the physiology of the buccal mucosa, an external mucus layer was prepared by a film method. A concentration of 100 mg/ml mucin was necessary to obtain a layer with a thickness of about 120–150 μm . Adding 2% glycerol to the aqueous mucus dispersion resulted in a mechanically stable layer (independent on the mucin-type). A glycerol content less than 2% led to an increased brittleness and shrinkage of the layer. The investigations of the different drying conditions revealed that a temperature of 4 $^{\circ}\text{C}$ was necessary to obtain mechanical stability, while drying at 37 $^{\circ}\text{C}$ and room temperature desiccated the layer excessively. Furthermore, the rheological properties of the mucin dispersions were evaluated. The viscosity of human mucin was inversely proportional to the shear rate, which indicated a non-Newtonian trait of biological fluid. The fluid behavior of the animal mucins was also dependent on the shear rate. Concerning the viscosity values at shear rates that would exist during swallowing or speech (i.e., 60–160 s^{-1}) [52], the porcine gastric mucus layer had a viscosity of 465 ± 26 mPa s at shear rates of 100 s^{-1} , whereas the viscosity of bovine submaxillary mucus layer was 132 ± 15 mPa s at the same shear rate. Human mucin exhibited a viscosity of 25 ± 1.2 mPa s, which was much lower than for animal mucin. These variations in viscosity could be attributed to the different mucin types and hence the different degree of glycosidic-bonds [53]. Highly glycosylated MAMs are able to bind a higher amount of water than un-glycosylated random coils, which implies a higher viscosity [54]. Since the investigated salivary mucin is extracted out of saliva, it comprises a high amount of secreted mucins (i.e., MUC 7), displaying a minor role in viscoelastic properties. Likewise, small differences in the concentrations of these mucins may be sufficient to cause changes in the viscoelastic behavior. However, Park et al. [36] observed only a marginal variation between the viscosity behaviors of different animal mucins compared to human mucin. These differences can be attributed to the low mucin concentrations used in their study.

The network formation properties were evaluated by SEM (Fig. 3). All tested mucins formed a 3-dimensional network. Comparing the human salivary (Fig. 3c) with the porcine gastric (Fig. 3a) mucus layer, the gel structure was similar, resulting in a network with parallel and crossing mucin fibers. The mucus mesh size could be determined with pore sizes up to 0.9 μm in diameter for the porcine gastric layer and 0.8 μm for the human mucin. In contrast, the bovine submaxillary layer (Fig. 3b) formed a network with a smaller mesh size (pores up to 0.4 μm). However, previous studies demonstrated that spherical viruses penetrated different mucus barriers and efficiently infiltrated mucosal tissues. The Norwalk (size 38 nm) and human papilloma (size 55 nm) viruses freely

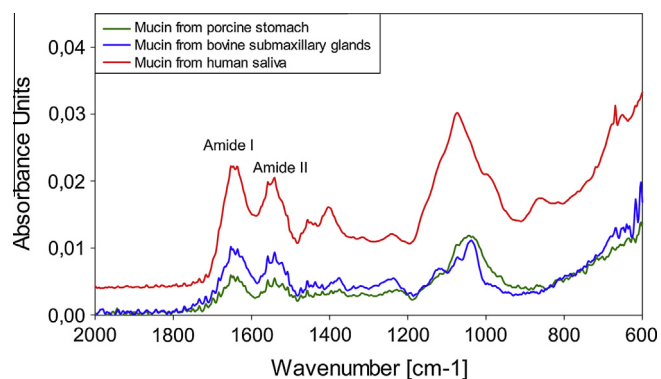


Fig. 1. FTIR absorbance spectrum of mucin from porcine stomach, bovine submaxillary glands, and mucin from human saliva. (For interpretation of the references to color in this figure legend, the reader is referred to the web version of this article.)

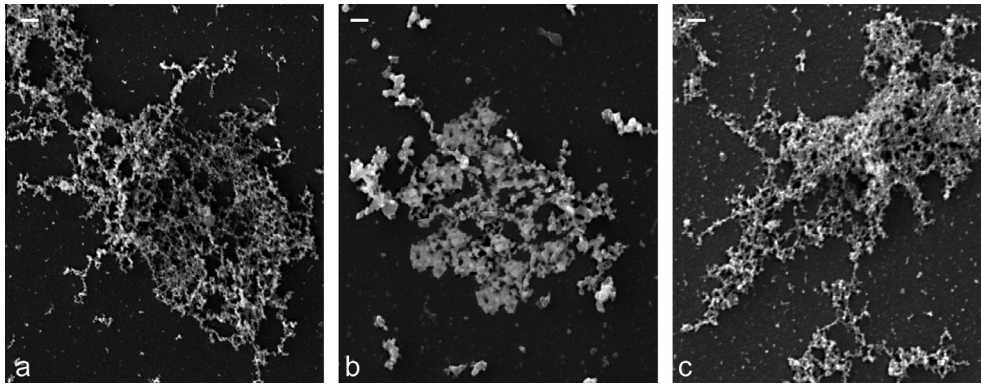


Fig. 2. SEM images showing the morphological structure of (a) porcine stomach, (b) bovine submaxillary glands, and (c) human salivary mucin fibers (scale bar = 1 μm).

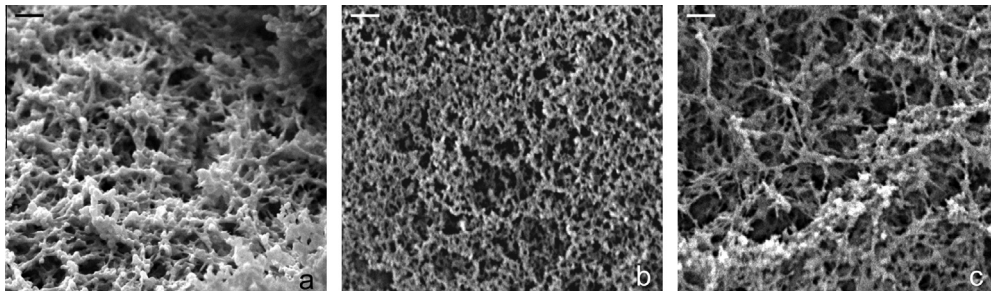


Fig. 3. SEM images of the mucus network formed by different types of mucins. (a) Porcine stomach mucus layer formed a mesh size with pores sizes up to 0.9 μm in diameter, (b) the network of the bovine submaxillary layer showed pore sizes up to 0.4 μm , and (c) the mesh size of human salivary mucin could be determined up to 0.8 μm (scale bar = 1 μm).

diffused through human cervical mucus barriers, suggesting a length scale up to 55 nm [55]. Additional findings showed that 180 nm viruses were also able to diffuse through the network. Recently, Lai et al. [56] demonstrated that polymeric nanoparticles with a size between 200 and 500 nm are also capable to traverse human cervical mucus. In the oral cavity, to our knowledge, the exact mucus mesh has not been evaluated so far. This is impeded by a lack of understanding of how (and partially which) mucins adhere onto the epithelial cells and form the oral glycocalyx. Thus, more investigations are necessary in future research.

3.3. Evaluation of the oral cell line

Two oral epithelial cell lines, TR 146 [21,23,24] and H 376 [57], were evaluated for confluence and integrity by measuring the Trans epithelial Electrical Resistance (TEER). As shown in Fig. 4, the H 376 cell line reached the highest effective TEER value on day 18 with $31.40 \pm 4.28 \Omega \text{cm}^2$. Subsequently, the integrity continuously decreased. Since the required tightness for transport was not reached, the H 376 cells were considered unsuitable for this study. The TR 146 cells reached the highest TEER values between day 27 and 28 with $50.02 \pm 2.87 \Omega \text{cm}^2$. Thereafter, a plateau was reached. Thus, this cell line was used for our experiments. The TR 146 cells were of human buccal epithelial origin and had a stratified epithelium with about 4 cell layers after 27 days in culture (see Fig. 5a and d). To evaluate if the high integrity was governed by tight junctions, the zonula occludens were highlighted with a fluorescence marker (data not shown). The data demonstrated that tight junctions were rare in this cell line, which is in agreement with the literature [21].

3.4. Development of the advanced in vitro model

Once the integrity of this cell line was maintained, the external mucus layers were deposited onto the confluent cell layers. The

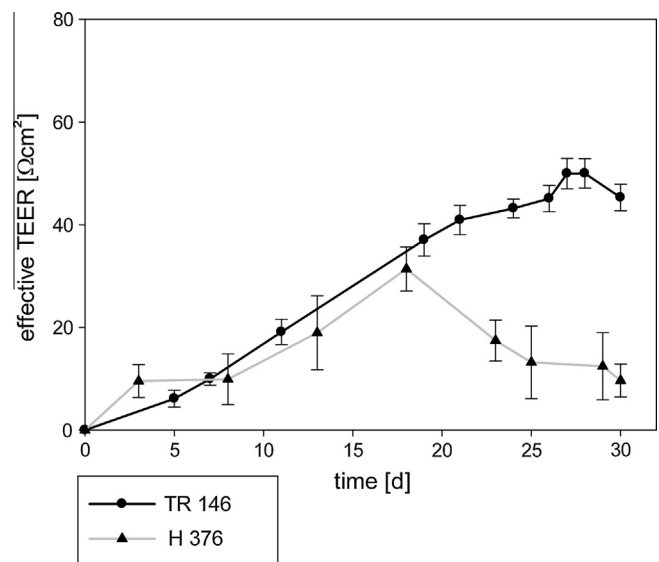


Fig. 4. TEER profiles of TR 146 and H 376 cells grown on Transwell® systems. The H 376 cells reached the highest TEER values on day 18 ($31.40 \pm 4.28 \Omega \text{cm}^2$) and the TR 146 cells between days 27 and 28 ($50.02 \pm 2.87 \Omega \text{cm}^2$). Data are presented as mean \pm SD ($n = 12$).

mucus adherent effects onto the cell surface were visualized by two different methods, that is, fluorescence microscopy and electron microscopy. For the fluorescent visualization of the mucin fibers, a suitable staining method was required. For a simple staining process, Acridine Orange (AO) was used as dye, taking the chemical properties of mucoglycoproteins into account. Since the mucus layer shows acidic properties, AO (pH sensitive) accumulated in

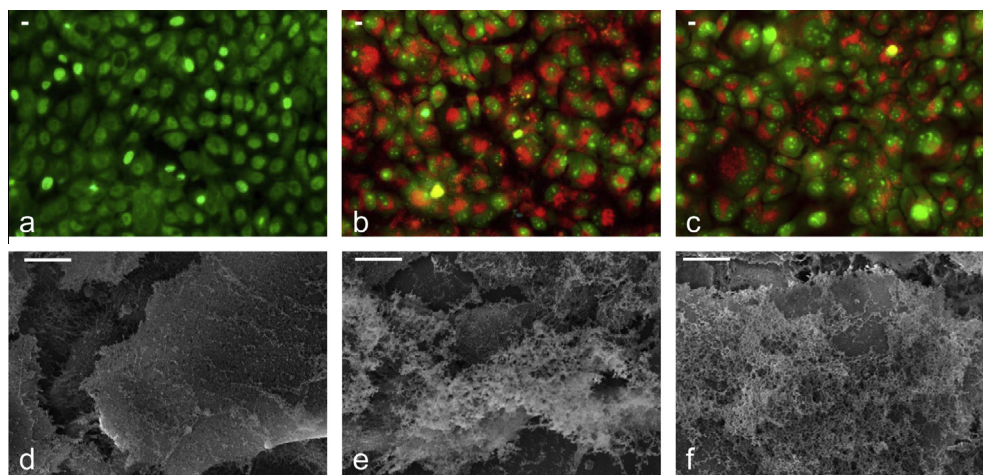


Fig. 5. Acridine Orange staining of (a) TR 146 cells, (b) TR 146 cells incubated with porcine gastric mucus layer, and (c) TR 146 cells incubated with bovine submaxillary mucus layer. The cytoplasm exhibit green emission, while the mucin fibers show red emission. SEM images of (d) TR 146 cells (control sample) and cells incubated with (e) porcine gastric mucus layer and (f) bovine submaxillary mucus layer (scale bar = 10 μm). (For interpretation of the references to color in this figure legend, the reader is referred to the web version of this article.)

the mucin fibers, inducing a shift from green emission to red emission (Fig. 5). The results displayed a detectable red fluorescence of the porcine (Fig. 5b) and bovine (Fig. 5c) mucus layer on the cell surface. In contrast, untreated cells exhibited only a green fluorescence (Fig. 5a). On the one hand, this suggests that viable cells can be distinguished from the mucus layer due to a green emission. On the other hand, adherent mucin fibers are detectable on the epithelial cells independent on the type of the external mucus layers (i.e., porcine gastric and bovine submaxillary mucus layer). To confirm these results, SEM images of TR 146 cells, incubated with the mucus layer, were provided. While no adherent mucoglycoproteins were detectable on the epithelial surface of the TR 146 cells (Fig. 5d), adherent porcine gastric (Fig. 5e) and bovine submaxillary (Fig. 5f) mucin fibers were clearly visible after incubation with the external layer. Hence, the adherent effects of the mucus layer could be verified by LSM and SEM. The mechanism behind the surface-adherence of the mucins could be attributed to the specific surface structure of the oral epithelium. Kullaa–Mikkonen [58] demonstrated that surfaces of superficial cells are comprised of ridge-like folds, so-called microplicae, which are also present in the cornea. There they maximize the absorbance of oxygen and nutrients and hold mucus on the cell surface [59]. Oral epithelial surfaces show strong affinity for mucins due to mucin binding proteins [60]. Recently, it was hypothesized by Asikainen et al. that both mechanisms are involved in the formation of an intact oral mucosal barrier complex [61].

To determine the viability of the advanced buccal in vitro model, the mitochondrial activity of TR 146 cells after incubation with the mucus layer was assessed. Toxic effects of the bovine mucus layer onto the cells could already be detected after 4 h. The viability decreased (dependent on time) to $71.5 \pm 3.3\%$ (Fig. 6). After 48-h incubation, a pronounced cytotoxic effect was determined with viability values less than 20%. This behavior can be explained by the morphological structure of bovine submaxillary mucin and the network formation of the layer. Once the layer is deposited on the cells and incubated with cell culture medium, the ionic strength increases and the mucin fibers become (time-dependent) stiff, compact coils. The stiffness is maintained due to repulsive electric forces of sialic side chains [48], showing an increasing integrity of the mucus layer (Fig. 3b). Due to the compact system, the cells could not be sufficiently supplied with the cell culture medium resulting in a decreased viability. In contrast, the mucus layer from porcine stomach displayed a mesh size up to 0.8 μm and showed no significant impact on the mitochondrial activity

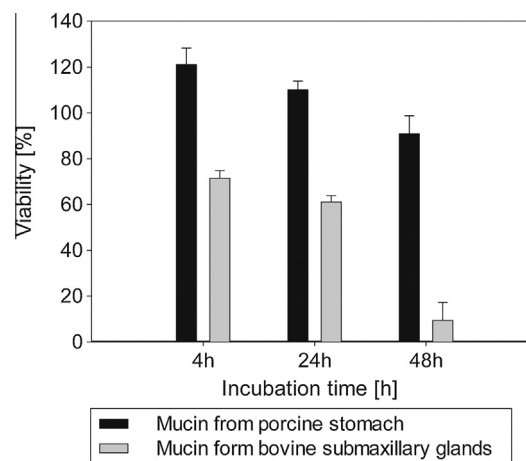


Fig. 6. MTS test of the advanced in vitro model. The cell viability was determined after incubation with the porcine mucus layer (black bar) and with the bovine mucus layer (gray bar).

within the tested time ($P > 0.05$). Thus, cells were adequately supplied and nearly 100% viability was maintained after 48 h. Based on these results, it can be concluded that the porcine gastric mucus layer did not affect the viability of the epithelial cells, and therefore, this layer was considered suitable for the advanced in vitro model.

3.5. Transport studies with polystyrene nanoparticles

One of the major advantages of in vitro research is that compared to animal models, cellular and sub-cellular functions can be studied easier in a simplified, biological model system. Nanoparticles are considered as new pharmaceutical formulations that can improve drug delivery. Yet, their design is impeded by a lack of understanding of how nanoparticles interact with the buccal mucosa. Recent studies demonstrated that the permeation/penetration of nanoparticles through/into the mucus layer and the epithelium was determined by the surface charge, the particle size, and the hydrophilicity [17]. Thus, an in vitro model that will be used for the evaluation of the penetration/permeation behavior of nanoparticles has to be standardized according to these aspects.

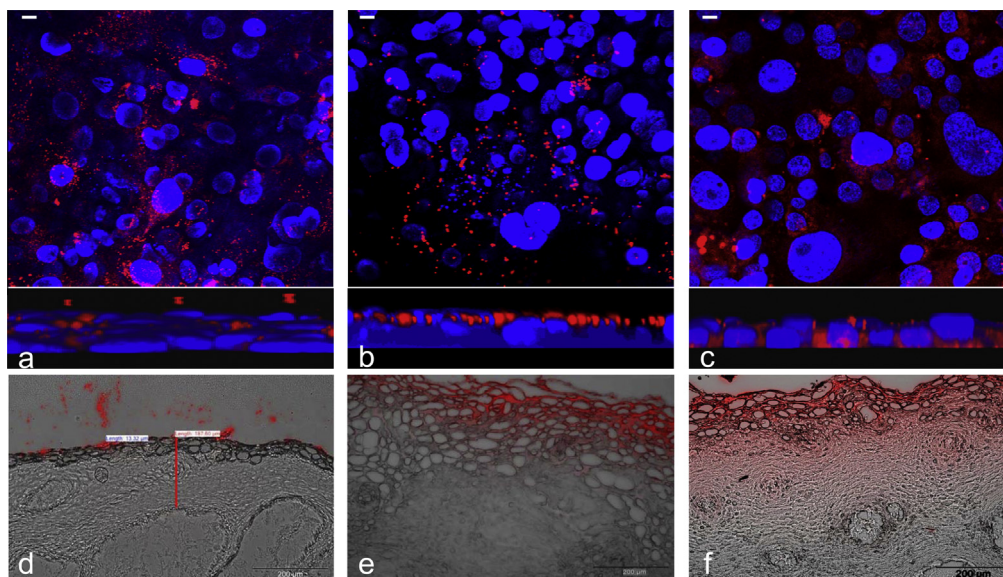


Fig. 7. Transport studies with the advanced buccal in vitro model in comparison with ex vivo experiments. The nuclei were stained with Hoechst (blue). (a) 200 nm CP particles (red) aggregated in the mucus layer of the in vitro model, (b) 200 nm AP particles (red), and (c) 200 nm PP particles (red) permeated the mucus layer and penetrated into the epithelium (scale bar = 10 μ m). Radial sections of the oral mucosa to determine the localization of (d) 200 nm CP, (e) 200 nm AP, and (f) 200 nm PP particles within the advance model (scale bar = 200 μ m). (For interpretation of the references to color in this figure legend, the reader is referred to the web version of this article.)

Therefore, in vitro and ex vivo transport studies were performed with hydrophilic 200 nm sized model particles of different charges (Fig. 7). The in vitro transport of negatively charged 200 nm CP particles (Fig. 7a) was hindered by the negatively charged mucin fibers and the particles aggregated within the network. Thus, CP 200 nm failed to penetrate into the epithelium. In contrast, positive 200 nm AP (Fig. 7b) and neutral 200 nm PP particles (Fig. 7c) were able to permeate the mucus layer and penetrated into the oral epithelium. The results from the ex vivo experiments confirmed the in vitro data. A total of 200 nm CP particles (Fig. 7d) were entrapped in the mucus layer. However, positive 200 nm (Fig. 7e) and neutral 200 nm particles (Fig. 7f) penetrated into deeper regions of the tissue. These results strongly suggest that in the buccal mucosa, the mucus layer together with the epithelium acts as a strong barrier for the uptake of nanoparticles. On the other hand, the results of the advanced in vitro model correlated well with the data from the ex vivo experiments, indicating a high reliability of the model.

4. Conclusions

In the current study, an advanced buccal in vitro model including oral epithelial TR 146 cells and an adherent mucus layer is developed. Our findings demonstrate that animal mucins, including porcine gastric and bovine submaxillary, reveal no chemical differences (relevant for the model) to human natural mucin. The mucus layers are prepared by a film method and adhere onto the epithelial TR 146 cells. Porcine gastric mucin maintains the viability of the system for more than 48 h. Nanoparticle transport studies correlate well with data from ex vivo permeability studies through porcine buccal mucosa indicating that our model is reliable. Additionally, the results strongly suggest that in the buccal mucosa, the mucus layer together with the epithelium acts as a strong barrier for the uptake of nanoparticles. The advanced buccal in vitro model is useful to study mucosal uptake and penetration of nanoparticles in the oral cavity.

Acknowledgments

This project was funded by EFRE A3-11.N-14/2010-5. The authors thank Christoph Neubauer of the Research Center Pharma-

ceutical Engineering Graz, Austria, for his assistance with FTIR and Claudia Meindl of the Medical University of Graz, Austria, for her assistance with fluorescence microscopy. Gertrud Havlicek and Rudolf Schmied, Medical University of Graz, are thanked for their assistance with SEM.

References

- [1] A.H. Shojaei, Buccal mucosa as a route for systemic drug delivery: a review, *J. Pharm. Pharm. Sci.* 1 (1998) 15–30.
- [2] C.A. Squier, P.W. Wertz, Permeability and the pathophysiology of oral mucosa, *Adv. Drug Deliv. Rev.* 12 (1993) 13–24.
- [3] A.C. Liang, L.-L.H. Chen, Fast-dissolving intraoral drug delivery systems, *Expert Opin. Ther. Pat.* 11 (2001) 981–986.
- [4] M. Dahiya, S. Saha, A.F. Shahiwala, A review on mouth dissolving films, *Curr. Drug Deliv.* 6 (2009) 469–476.
- [5] V.F. Patel, F. Liu, M.B. Brown, Advances in oral transmucosal drug delivery, *J. Control. Release* 153 (2011) 106–116.
- [6] J. Swarbrick, *Drug Delivery to the Oral Cavity: Molecules to Market*, Informa Healthcare, New York, London, 2010, pp. 1–40.
- [7] C.A. Squier, M.J. Kremer, Biology of oral mucosa and esophagus, *J. Natl. Cancer Inst. Monogr.* (2001) 7–15.
- [8] R.B. Gandhi, J.R. Robinson, Oral cavity as a site for bioadhesive drug delivery, *Adv. Drug Deliv. Rev.* 13 (1994) 43–74.
- [9] D. Harris, J.R. Robinson, Drug delivery via the mucous membranes of the oral cavity, *J. Pharm. Sci.* 81 (1992) 1–10.
- [10] L.M. Collins, C. Dawes, The surface area of the adult human mouth and thickness of the salivary film covering the teeth and oral mucosa, *J. Dent. Res.* 66 (1987) 1300–1302.
- [11] A.H. Beckett, E.J. Triggs, Buccal absorption of basic drugs and its application as an in vivo model of passive drug transfer through lipid membranes, *J. Pharm. Pharmacol.* 19 (1967) 31–41. Suppl.
- [12] M.M. Veillard, M.A. Longer, T.W. Martens, J.R. Robinson, Preliminary studies of oral mucosal delivery of peptide drugs, *J. Control. Release* 6 (1987) 123–131.
- [13] J.C. Hoffmann, N.N. Pawlowski, A.A. Kuhl, W. Hohne, M. Zeitz, Animal models of inflammatory bowel disease: an overview, *Pathobiology* 70 (2002) 121–130.
- [14] C.A. Lesch, C.A. Squier, A. Cruchley, D.M. Williams, P. Speight, The permeability of human oral mucosa and skin to water, *J. Dent. Res.* 68 (1989) 1345–1349.
- [15] H. Zhang, J.R. Robinson, Routes of drug transport across oral mucosa, in: M.J. Rathbone (Ed.), *Oral Mucosal Drug Delivery*, Marcel Dekker, New York, 1996, pp. 51–63.
- [16] P.W. Wertz, C.A. Squier, Cellular and molecular basis of barrier function in oral epithelium, *Crit. Rev. Ther. Drug Carrier Syst.* 8 (1991) 237–269.
- [17] E. Roblegg, E. Fröhlich, C. Meindl, B. Teubl, M. Zaversky, A. Zimmer, Evaluation of a physiological in vitro system to study the transport of nanoparticles through the buccal mucosa, *Nanotoxicology* 6 (2011) 399–413.
- [18] A. des Rieux, V. Fievez, I. Théate, J. Mast, V. Préat, Y.-J. Schneider, An improved in vitro model of human intestinal follicle-associated epithelium to study nanoparticle transport by M cells, *Eur. J. Pharm. Sci.* 30 (2007) 380–391.

- [19] A. des Rieux, E.G.E. Ragnarsson, E. Gullberg, V. Pr eat, Y.-J. Schneider, P. Artursson, Transport of nanoparticles across an in vitro model of the human intestinal follicle associated epithelium, *Eur. J. Pharm. Sci.* 25 (2005) 455–465.
- [20] N.R. Yacobi, L. DeMaio, J. Xie, S.F. Hamm-Alvarez, Z. Borok, K.-J. Kim, E.D. Crandall, Polystyrene nanoparticle trafficking across alveolar epithelium, *Nanomed. Nanotechnol. Biol. Med.* 4 (2008) 139–145.
- [21] J. Jacobsen, B. van Deurs, M. Pedersen, M.R.M. Rassing, TR146 cells grown on filters as a model for human buccal epithelium: I. Morphology, growth, barrier properties, and permeability, *Int. J. Pharm.* 125 (1995) 165–184.
- [22] H.T. Rupniak, C. Rowlatt, E.B. Lane, J.G. Steele, L.K. Trejdosiewicz, B. Laskiewicz, S. Povey, B.T. Hill, Characteristics of four new human cell lines derived from squamous cell carcinomas of the head and neck, *J. Natl Cancer Inst.* 75 (1985) 621–635.
- [23] H.M. Nielsen, M.R. Rassing, TR146 cells grown on filters as a model of human buccal epithelium: III. Permeability enhancement by different pH values, different osmolality values, and bile salts, *Int. J. Pharm.* 185 (1999) 215–225.
- [24] H.M. Nielsen, M.R. Rassing, TR146 cells grown on filters as a model of human buccal epithelium: IV. Permeability of water, mannitol, testosterone and β^2 -adrenoceptor antagonists. Comparison to human, monkey and porcine buccal mucosa, *Int. J. Pharm.* 194 (2000) 155–167.
- [25] A.B.R. Thomson, J.M. Dietschy, Derivation of the equations that describe the effects of unstirred water layers on the kinetic parameters of active transport processes in the intestine, *J. Theor. Biol.* 64 (1977) 277–294.
- [26] M.M. Veillard, Buccal and gastrointestinal drug delivery systems, in: R. Gurny, H.E. Junginger (Eds.), *Bioadhesion – Possibilities and Future Trends*, wissenschaftliche Verlagsgesellschaft mbH, Stuttgart, 1990.
- [27] V.L. Bykov, The tissue and cell defense mechanisms of the oral mucosa, *Morfologija* 110 (1996) 14–24.
- [28] V.L. Bykov, The functional morphology of the epithelial barrier of the oral mucosa, *Stomatologija (Mosk)* 76 (1997) 12–17.
- [29] P.A. Nielsen, E.P. Bennett, H.H. Wandall, M.H. Therkildsen, J. Hannibal, H. Clausen, Identification of a major human high molecular weight salivary mucin (MG1) as tracheobronchial mucin MUC5B, *Glycobiology* 7 (1997) 413–419.
- [30] C. Wickstrom, J.R. Davies, G.V. Eriksen, E.C. Veerman, I. Carlstedt, MUC5B is a major gel-forming, oligomeric mucin from human salivary gland, respiratory tract and endocervix: identification of glycoforms and C-terminal cleavage, *Biochem. J.* 334 (Pt 3) (1998) 685–693.
- [31] F. Lagerlof, C. Dawes, The volume of saliva in the mouth before and after swallowing, *J. Dent. Res.* 63 (1984) 618–621.
- [32] R. Ghandi, J. Robinson, Bioadhesion in drug delivery, *Ind. J. Pharm. Sci.* 3 (1988) 145–152.
- [33] P.J. Thomson, C.S. Potten, D.R. Appleton, Mapping dynamic epithelial cell proliferative activity within the oral cavity of man: a new insight into carcinogenesis?, *Br J. Oral Maxillofac. Surg.* 37 (1999) 377–383.
- [34] P.W. Wertz, D.C. Swartzendruber, C.A. Squier, Regional variation in the structure and permeability of oral mucosa and skin, *Adv. Drug Deliv. Rev.* 12 (1993) 1–12.
- [35] S. Law, P.W. Wertz, D.C. Swartzendruber, C.A. Squier, Regional variation in content, composition and organization of porcine epithelial barrier lipids revealed by thin-layer chromatography and transmission electron microscopy, *Arch. Oral Biol.* 40 (1995) 1085–1091.
- [36] M.S. Park, J.W. Chung, Y.K. Kim, S.C. Chung, H.S. Kho, Viscosity and wettability of animal mucin solutions and human saliva, *Oral Dis.* 13 (2007) 181–186.
- [37] J. Schaffer, Ver nderungen an Gewebeelementen durch einseitige Wirkung der Fixierungsfl ssigkeit und Allgemeines  ber Fixierung, *Anat. Anz.* 51 (1918) 353–398.
- [38] B. Liu, J.R. Lague, D.P. Nunes, P. Toselli, F.G. Oppenheim, R.V. Soares, R.F. Troxler, G.D. Offner, Expression of membrane-associated mucins MUC1 and MUC4 in major human salivary glands, *J. Histochem. Cytochem.* 50 (2002) 811–820.
- [39] A. Sengupta, D. Valdramidou, S. Huntley, S.J. Hicks, S.D. Carrington, A.P. Corfield, Distribution of MUC1 in the normal human oral cavity is localized to the ducts of minor salivary glands, *Arch. Oral Biol.* 46 (2001) 529–538.
- [40] P.A. Nielsen, U. Mandel, M.H. Therkildsen, H. Clausen, Differential expression of human high-molecular-weight salivary mucin (MG1) and low-molecular-weight salivary mucin (MG2), *J. Dent. Res.* 75 (1996) 1820–1826.
- [41] E.C. Veerman, P.A. van den Keybus, A. Vissink, A.V. Nieuw Amerongen, Human glandular salivas: their separate collection and analysis, *Eur. J. Oral Sci.* 104 (1996) 346–352.
- [42] J.G.M. Bolscher, J. Groenink, J.S. van der Kwaak, P.A.M. van den Keijbus, W. van't Hof, E.C.I. Veerman, A.V. Nieuw Amerongen, Detection and quantification of MUC7 in submandibular, sublingual, palatine, and labial saliva by anti-peptide antiserum, *J. Dent. Res.* 78 (1999) 1362–1369.
- [43] A. Vissink, H.P. De Jong, H.J. Busscher, J. Arends, E.J. Gravenmade, Wetting properties of human saliva and saliva substitutes, *J. Dent. Res.* 65 (1986) 1121–1124.
- [44] A. Vissink, H.A. Waterman, E.J. s-Gravenmade, A.K. Panders, A. Vermey, Rheological properties of saliva substitutes containing mucin, carboxymethylcellulose or polyethylenoxide, *J. Oral Pathol.* 13 (1984) 22–28.
- [45] A. Vissink, E.J. s-Gravenmade, A.K. Panders, A. Vermey, J.K. Petersen, L.L. Visch, R.M. Schaub, A clinical comparison between commercially available mucin- and CMC-containing saliva substitutes, *Int. J. Oral Surg.* 12 (1983) 232–238.
- [46] A. Elliott, E.J. Ambrose, Structure of synthetic polypeptides, *Nature* 165 (1950) 921–922.
- [47] M. Jackson, H.H. Mantsch, The use and misuse of FTIR spectroscopy in the determination of protein structure, *Crit. Rev. Biochem. Mol. Biol.* 30 (1995) 95–120.
- [48] F.A. Bettelheim, S.K. Dey, Molecular parameters of submaxillary mucins, *Arch. Biochem. Biophys.* 109 (1965) 259–265.
- [49] H. Nordman, J.R. Davies, G. Lindell, C. de Bolos, F. Real, I. Carlstedt, Gastric MUC5AC and MUC6 are large oligomeric mucins that differ in size, glycosylation and tissue distribution, *Biochem. J.* 364 (2002) 191–200.
- [50] B.J.-W. Van Klinken, J. Dekker, S.A. Van Gool, J. Van Marle, H.A. B ller, A.W.C. Einerhand, MUC5B is the prominent mucin in human gallbladder and is also expressed in a subset of colonic goblet cells, *Am. J. Physiol.-Gastr. L.* 274 (1998) G871–G878.
- [51] M.A. McGuckin, S.K. Lind n, P. Sutton, T.H. Florin, Mucin dynamics and enteric pathogens, *Nat. Rev. Micro.* 9 (2011) 265–278.
- [52] R.T. Balmer, S.R. Hirsch, The non-Newtonian behaviour of human saliva, *AIChE Symp. Ser. Biorheol.* 181 (74) (1978) 125–129.
- [53] F.A. Meyer, A. Silberberg, Structure and function of mucus, in: *Ciba Foundation Symposium 54 – Respiratory Tract Mucus*, John Wiley & Sons, Ltd., 2008, pp. 203–218.
- [54] C.L. Hattrup, S.J. Gendler, Structure and function of the cell surface (tethered) mucins, *Annu. Rev. Physiol.* 70 (2008) 431–457.
- [55] S.S. Olmsted, J.L. Padgett, A.I. Yudin, K.J. Whaley, T.R. Moench, R.A. Cone, Diffusion of macromolecules and virus-like particles in human cervical mucus, *Biophys. J.* 81 (2001) 1930–1937.
- [56] S.K. Lai, D.E. O'Hanlon, S. Harrold, S.T. Man, Y.Y. Wang, R. Cone, J. Hanes, Rapid transport of large polymeric nanoparticles in fresh undiluted human mucus, *Proc. Natl. Acad. Sci. USA* 104 (2007) 1482–1487.
- [57] S.S. Prime, S.V. Nixon, I.J. Crane, A. Stone, J.B. Matthews, N.J. Maitland, L. Remnant, S.K. Powell, S.M. Game, C. Scully, The behaviour of human oral squamous cell carcinoma in cell culture, *J. Pathol.* 160 (1990) 259–269.
- [58] A. Kullaa-Mikkonen, Scanning electron microscopic study of surface of human oral mucosa, *Eur. J. Oral Sci.* 94 (1986) 50–56.
- [59] I.K. Gipson, Distribution of mucins at the ocular surface, *Exp. Eye Res.* 78 (2004) 379–388.
- [60] A. Slomiany, H. Nishikawa, B.L. Slomiany, Screening and modulation of extracellular signals by mucous barrier. Serum glycosylphosphatidylinositol phospholipase D (GPI-PLD) releases protective mucous barrier from oral mucosa, *J. Physiol. Pharmacol.* 53 (2002) 21–38.
- [61] P. Asikainen, T.J. Ruotsalainen, J.J. Mikkonen, A. Koistinen, C. Ten Bruggenkate, A.M. Kullaa, The defence architecture of the superficial cells of the oral mucosa, *Med. Hypotheses* 78 (2012) 790–792.